

Enhancing the accuracy of automatic eddy detection

J. Yi et al.

This discussion paper is/has been under review for the journal Ocean Science (OS).  
Please refer to the corresponding final paper in OS if available.

# Enhancing the accuracy of automatic eddy detection and the capability of recognizing the multi-core structures from maps of sea level anomaly

J. Yi<sup>1</sup>, Y. Du<sup>1</sup>, Z. He<sup>2,3</sup>, and C. Zhou<sup>1</sup>

<sup>1</sup>State Key Laboratory of Resources and Environmental Information System, Institute of Geographic Science and Natural Resources Research, Chinese Academy of Sciences, Beijing 100101, China

<sup>2</sup>State Key Laboratory of Tropical Oceanography (LTO), South China Sea Institute of Oceanology, Chinese Academy of Sciences, Guangzhou 510301, Guangdong, China

<sup>3</sup>College of Ocean and Earth Sciences, Xiamen University, Xiamen 361005, China

Received: 5 April 2013 – Accepted: 23 April 2013 – Published: 29 April 2013

Correspondence to: Y. Du (duyy@lreis.ac.cn)

Published by Copernicus Publications on behalf of the European Geosciences Union.

Title Page

Abstract

Introduction

Conclusions

References

Tables

Figures

⏪

⏩

◀

▶

Back

Close

Full Screen / Esc

Printer-friendly Version

Interactive Discussion

## Abstract

Automated methods are important for automatically detecting mesoscale eddies in large volumes of altimeter data. While many algorithms have been proposed in the past, this paper presents a new method, called Hybrid Detection (HD), to enhance the eddy detection accuracy and the capability of recognizing eddies' multi-core structures from maps of sea level anomaly (SLA) by integrating the ideas of the Okubo–Weiss (OW) method and the sea-surface-height-based (SSH-based) method, two well-known eddy detection algorithms. Detection evaluation using an objective validation protocol shows that the HD method owns ~96.6% successful detection rate and ~14.2% excessive detection rate, which outperforms the OW method and other methods that identify eddies by SLA extrema and confirms the improvement in detection accuracy. The capability of recognizing multi-core structures and its significance in tracking eddies' splitting or merging events have been well illustrated by comparing with other detection algorithms and historical studies.

## 1 Introduction

Mesoscale eddies play an important role in ocean circulation as well as in heat and mass transport (McWilliams, 2008; Nencioli et al., 2010). With the development of observation technology, automated detection methods are essential for understanding the complex movements and dynamic characteristics of mesoscale eddies in large volumes of altimeter data. In the Eulerian scheme (distinguished from Lagrangian detection scheme using drifting trajectory data, Dong et al., 2011), existing eddy detection methods can be categorized into three classes: (1) those based on physical parameter, (2) those based on flow geometry, and (3) those based on sea surface height anomaly (SSHA).

Among the first category, the Okubo–Weiss (OW) approach (Okubo, 1970; Weiss, 1991) is the most widely used. The physical parameter  $W$  is computed from the

OSD

10, 825–851, 2013

## Enhancing the accuracy of automatic eddy detection

J. Yi et al.

Title Page

Abstract

Introduction

Conclusions

References

Tables

Figures

⏪

⏩

◀

▶

Back

Close

Full Screen / Esc

Printer-friendly Version

Interactive Discussion





## Enhancing the accuracy of automatic eddy detection

J. Yi et al.

Title Page

Abstract

Introduction

Conclusions

References

Tables

Figures

⏪

⏩

◀

▶

Back

Close

Full Screen / Esc

Printer-friendly Version

Interactive Discussion

delineate eddies' dimensions. An objective validation protocol which has been used by Chaigneau et al. (2008) and Nencioli et al. (2010) is adopted to measure the detection quality of the HD method. In addition, the detection results of different algorithms has been compared to illustrate the performance of HD and its capability of capturing multi-core structures. Nan et al. (2010)'s study on three anticyclonic eddies among which splitting and merging events had been observed is used to verify HD's detection results and to demonstrate the significance of recognizing multi-core structures.

The rest of the paper is organized as follows: Sect. 2 introduces the altimetry data and the detailed procedures of the HD method; Sect. 3 presents the results and discussion of HD's detection evaluation, methods comparisons, and historical verifications; and the final section provides the conclusions.

## 2 Data and method

### 2.1 Altimetry data

As combining data from different satellite missions improves the estimation of mesoscale signals (Traon and Dibarboure, 1999; Chelton and Schlax, 2003; Pascual et al., 2006), SLA dataset (October 1992 to April 2012) of the AVISO (<http://www.aviso.oceanobs.com>) Reference Series delayed-time altimeter products merging TOPEX/Poseidon (T/P), Jason-1, ERS-1/2, and Envisat data (Ducet et al., 2000) was used to identify mesoscale eddies. This merged altimeter dataset consists of weekly SLA maps computed with respect to a seven-year mean and resampled on a  $1/3^\circ \times 1/3^\circ$  Mercator grid.

### 2.2 Eddy detection methodology

Two major procedures are involved in conventional eddy identification: first is to recognize the center of eddy, second is to extract the boundary. But to identify the multi-core structures, HD includes an additional procedure to determine if the eddies constitute

any multi-core structure of which the closed boundary contains more than one local extrema of the same polarity. So the methodology of the new method has three steps: (1) identify eddy centers; (2) define and extract eddy boundaries; and (3) distinguish multi-core structures.

### 2.2.1 Step 1: a hybrid way to identify eddy centers

The OW method identifies eddies by the criterion that parameter  $W$  less than  $-0.2\sigma_w$  ( $\sigma_w$  is the spatial standard deviation of  $W$ ). This criterion, however, may include noises that are overly detected as eddies and therefore diminishes the identification quality. Another criterion that many methods adopted to detect eddies is that at least one local SLA or SSHA extrema is located within eddies' boundaries. The threshold-free SSH-based method (Chelton et al., 2011), for instance, requires qualified eddies to contain at least one local minimum or maximum. And Chaigneau et al. (2008) took local SLA minima or maxima as possible cyclonic or anticyclonic eddy centers. It is noteworthy, however, that noises on SSHA or SLA fields may also form local extrema that induce excessive detections. So, to combine the two criteria together in detecting ocean eddies would be a better resolution of reducing excessive detections and efficiently enhancing the identification accuracy. Consequently, this study implemented these two criteria into the HD method. And to avoid confusion, the local extrema of SLA in eddies are referred to as "eddy centers" while the connected regions where  $W < -0.2\sigma_w$  are referred to as "eddy cores".

Figure 1 shows the details of the step 1. Each global SLA map is first clipped to the study region (e.g. the South China Sea). Then, the program calculates the  $W$  parameter and searches for the local extrema in separate on that clipped SLA. Regions where  $W < -0.2\sigma_w$  are extracted as eddy cores. And local SLA extrema searched out by a  $3 \times 3$  grid moving window (the smallest scale) will be qualified as eddy centers only if they are located within any core areas.

In this procedure, extra restrictions can be flexibly added based on the data quality of different study regions. In the South China Sea, for example, eddy centers located

Enhancing the accuracy of automatic eddy detection

J. Yi et al.

Title Page

Abstract

Introduction

Conclusions

References

Tables

Figures

⏪

⏩

◀

▶

Back

Close

Full Screen / Esc

Printer-friendly Version

Interactive Discussion



over water depths shallower than 100 m are removed due to the alias from tides and internal waves contained in the SLA data over the shallow shelf area (Yuan et al., 2006). In addition, smoothing algorithm, like half-power filter (Chelton et al., 2011) or Hanning filter (Penven et al., 2005), can also be added to reduce the noises in  $W$  field. But to avoid removing any physical information, this study applied no smoothing algorithms.

## 2.2.2 Step 2: definition and extraction of eddy boundaries

Existing algorithms lack a unified definition of eddy boundaries, and detection results can vary significantly depending on the rules for extracting the boundary (Nencioli et al., 2010). The OW method defines enclosed regions where  $W$  values satisfy the criterion as eddies. However, this criterion is restricted to the core of the vortices and may underestimate eddies' dimensions (Basdevant and Philipovitch, 1994). The WA method and the VG method represent eddies' boundaries by streamlines which make better approximation of eddies' shapes. And given the good agreement with streamlines, the SSH-based method takes the outermost closed contours of SSHA as eddy boundaries. The HD method in this paper also uses SLA contours to represent eddy boundaries, but the "outmost" criterion is further refined to make the boundary extraction more sensible. The detail procedures are showed in Fig. 2.

First, a series of contours of SLA are generated with increments of 0.5 cm, although 1 cm increments had been confirmed good enough to resolve the eddies with compact interiors (Chelton et al., 2011). The smaller increment is preferred for it makes the contours more precise and therefore the extracted eddy boundaries more correct. Contours that are unclosed or have a diameter less than 500 km are removed from the dataset.

Second, the eddy centers and cores identified in the step 1 are combined to decide which contours surrounding the eddy centers should be their corresponding boundaries. For each eddy center, the smallest contour that covers its core area is regarded as the qualified boundary. This definition improves the approximation of eddies' shapes

## Enhancing the accuracy of automatic eddy detection

J. Yi et al.

Title Page

Abstract

Introduction

Conclusions

References

Tables

Figures

⏪

⏩

◀

▶

Back

Close

Full Screen / Esc

Printer-friendly Version

Interactive Discussion

while choosing the outmost closed contours as boundaries tend to enlarge the dimensions. Figure 3a illustrates the difference between the two criteria.

It is noteworthy that some special situations may occur during the process of extracting eddies' boundaries. For instance, it is possible that eddies may have no contours completely covering their core areas (Fig. 3b), or even no closed contours intersected with (Fig. 3c). In the former case, eddies' boundaries are defined by the outermost closed contour that have intersections with the core areas, while in the latter case, eddies' dimensions are defined by the cores, just as the OW method does. While some may argue about the existence of these weak eddies in the latter case, this study retains them during the identification process for that they may be in the immature or unstable stages (e.g. forming or disappearing) during their long evolution processes and removing them will inevitably lead to fragments of their original processes when they are tracked. Figure 3d illustrate another case that eddy boundaries contain extra local extrema but not qualified eddy centers. In such cases, the boundaries usually improperly enlarge the dimensions so that are removed before the boundary extraction procedure. Moreover, contours contain two or more eddy centers that have opposite polarities are also discarded.

### 2.2.3 Step 3: multi-core recognition and boundary restoration

The multi-core structures of eddies, which have two or more close eddies of the same polarity within the boundaries, represent the important transitional stages of their lives in which component eddies may be experiencing splitting, merging or other energy-transferring interactions, although they were few mentioned and had no rigid definition in previous studies. The SSH-based can yield the multi-core structures, but it failed to record their shapes and track their evolution processes. The HD method developed in this study attempts to first fully recognize eddies' multi-core structures and lay the foundations for further addressing the difficulties they brought to tracking algorithms. After step 2, every eddy center has been associated with only one certain boundary.

## Enhancing the accuracy of automatic eddy detection

J. Yi et al.

Title Page

Abstract

Introduction

Conclusions

References

Tables

Figures



Back

Close

Full Screen / Esc

Printer-friendly Version

Interactive Discussion

So, in this step, we define that any eddy's boundary that contains more than one center forms a multi-core structure.

In order to distinguish and describe the composite whole structures and the component eddies, we define the boundaries of the whole structures as "state borders" and the boundaries of the component eddies as "footprint borders". The state border is represented by the outermost boundary of the component eddies and the footprint border is represented by the outermost contour that contains only one eddy center. After recognizing multi-core structures, the procedure needs to check every eddy's boundary and extract the state borders and footprint borders. For example, in the Fig. 4a, after step 2, sub-eddy C's boundary was found the outmost boundary containing sub-eddy A and B, and therefore it should be altered into the state border. In the meantime, sub-eddy B's boundary conflicts the definition of footprint border for it contains eddy A, so that subsequent restorations are needed to assign the correct boundary. Figure 4b shows the correct borders of the multi-core structure and its component eddies after the boundary restoration based on the definitions of state borders and footprint borders.

### 3 Results and discussion

#### 3.1 Accuracy evaluation

The accuracy is an important measure of the eddy identification quality. According to the validation protocol in Chaigneau et al. (2008), two quantities can be used for evaluating the accuracy of identification algorithms: the success of detection rate (SDR)

## Enhancing the accuracy of automatic eddy detection

J. Yi et al.

Title Page

Abstract

Introduction

Conclusions

References

Tables

Figures

⏪

⏩

◀

▶

Back

Close

Full Screen / Esc

Printer-friendly Version

Interactive Discussion



and the excess of detection rate (EDR). Definitions are showed as follows:

$$\text{SDR} = \frac{N_c}{N_e} \quad (1)$$

$$\text{EDR} = \frac{N_{\text{om}}}{N_e} \quad (2)$$

5 where  $N_c$  corresponds to the number of the eddies identified by both experts and the automated algorithm,  $N_e$  corresponds to the number of the eddies only identified by the experts, and  $N_{\text{om}}$  corresponds to the number of the eddies only identified by the algorithm.

10 This study randomly selected ten SLA maps of SCS (100–125° E; 5–26° N) from 1992 to 2012 to compute the SDR and the EDR according to the evaluation protocol. And five experts were invited to manually detect the eddies on these sample maps in order to gain the expert references. However, since subjective bias may exist between different experts' detections, it is necessary to estimate the uncertainties and derive a unified result for comparisons. So we introduce another index, the ratio of inconsistency (RI), to do the evaluation. The definition is showed as follows:

$$\text{RI}_i = \frac{|N_i - N_{\text{ce}}|}{N_{\text{ce}}} \quad (3)$$

15 where  $\text{RI}_i$  denotes the inconsistency rate of expert  $i$ .  $N_i$  is the number of the eddies identified by expert  $i$  and  $N_{\text{ce}}$  is the number of the eddies that are commonly recognized by at least three experts.  $N_i$  may be less than  $N_{\text{ce}}$  if most correct eddies are missed by the expert. So to avoid negative values, we only compute the absolute value of RI.

20 Figure 5a shows the comparison between expert detection (circles) and the HD result (dots) on 9 May 2007, SCS. There are 25 eddies ( $N_e = 25$ ) detected by the experts on this dataset (12 cyclonic and 13 anticyclonic). Four eddies were overly detected ( $N_{\text{om}} = 4$ ) and one was missed ( $N_c = 24$ ) by the HD. So, according to the definition, SDR = 96.0 % and EDR = 16.0 % in this experiment.

25

**Enhancing the accuracy of automatic eddy detection**

J. Yi et al.

Title Page

Abstract

Introduction

Conclusions

References

Tables

Figures

⏪

⏩

◀

▶

Back

Close

Full Screen / Esc

Printer-friendly Version

Interactive Discussion



## Enhancing the accuracy of automatic eddy detection

J. Yi et al.

Title Page

Abstract

Introduction

Conclusions

References

Tables

Figures

⏪

⏩

◀

▶

Back

Close

Full Screen / Esc

Printer-friendly Version

Interactive Discussion



Table 1 presents the evaluation results of the ten random test on SLA maps. About 22 eddies were identified every SLA map by the experts on average. The mean inconsistency rate suggests that  $\sim 20.7\%$  of the eddies are suspicious and raise disagreements among the manual detection process, and can be regarded as an upper bound of the acceptable tolerance for detection errors. The OW method and the methods which use SLA local extrema (e.g. the WA method) to identify eddy centers were also evaluated in Table 1 in order to compare with the HD method.

The results show that all the detection methods have relatively high SDRs. The methods using SLA local extrema to identify eddies maintain 100% SDR on every map, which confirms that the SLA local extrema are the necessary evidences for the existence of eddies. The SDRs of the OW method and the HD method are both equal to  $\sim 96.6\%$  on average;  $\sim 3.4\%$  of the eddies failed to be recognized by either OW or HD. Further examination reveals that these overlooked eddies did not locate in the intense vorticity regions (where  $W < -0.2\sigma_w$ ) but nearby (Fig. 5b), and were hence excluded from the qualified eddy centers identified by the HD method.

Second, the EDRs of different methods in the results vary wildly. The OW's EDR is high up to  $\sim 70.3\%$  on average and even exceeds 100% on single experiments (e.g. on 19 May 2007), which evidences the over-detection weakness of the OW method. The average EDR of SLA-extremum-based method ( $\sim 36.8\%$ ) is much lower than that of OW, which agrees with the validation results in (Chaigneau et al., 2008) and confirms that the WA method is more accurate. The HD method has the lowest EDR no matter in single experiments or on average, which substantiates that the integration of OW and SSH-based method gains effective improvements in detection accuracy. In addition, the average EDR of HD ( $\sim 14.2\%$ ) is under the tolerance bound (20.7%) of acceptable detection errors, which again confirms the effectiveness and the feasibility in practice of this hybrid method. Further investigation shows that the  $\sim 14.2\%$  excessively detected eddies can be ascribe to two major reasons: most of them (1) constitute as a part of multi-core structures (Fig. 5c); or (2) are located near the study region's border (Fig. 5d). And both cases tend to be overlooked in manual detection.

### 3.2 Comparison with other eddy detection methods

This study employed different detection algorithms to identify the eddies in eastern South-Pacific Ocean (3–20° S; 70–90° W) on the SLA map of 8 December 2004, in order to make a comparison study and reveal every method's characteristics in eddy detection. Figure 6 shows the manual detection result as well as every method's result on that date.

The comparison shows that, the OW method has a 100 % SDR, but the EDR is still relatively high (~ 71.9 %) because of the excessive detections. And the dimensions of the eddies are generally smaller than those depicted by the experts. The WA method that Chaigneau et al. (2008) adapted takes the SLA local extrema as eddy centers, so that the SDR is high up to 93.8 % while the EDR is less than 25.1 %. The SSH-based detection result is similar with that of WA except for the multi-core structure formed by two close cyclonic eddies located around (15° S, 78° W). The SDR (78.1 %) and the EDR (28.1 %) of the SSH-based method are not as good as those of WA for some eddies located along the coastline or near the study region's borders where the SLA contours are not closed are missed by this method. In the result of VG, the number of recognized eddies is much less and the detection accuracy (SDR = 50.0 %, EDR = 6.3 %) is poor compared to Nencioli et al. (2010)'s study in which high resolution datasets were used. The limited resolution of the SLA datasets could be the main reasons for this performance. The detection accuracy of the HD method (SDR = 90.6 %, EDR = 25.0 %), though not the best, is acceptable in this analysis. Careful examinations reveal that the overly detected eddies all satisfy the HD's detection criteria, though most of them are of small dimensions and weak SLA signals and are thus excluded by the experts. Moreover, HD has recognized three multi-core structures and one of them corresponds with the cyclonic two-core structure identified by the SSH-based method. The composite structures of these eddies indicate close relationships between them during their evolution processes.

In sum, this comparison study, although hardly proves which method perform the best, well distinguishes each method's detection characteristics. And the HD method not only maintains accurate detection performance but also shows the capability of recognizing multi-core structures of eddies.

### 3.3 Detection verification

The eddies studied by previous literature provide good references for eddy verifications of automatic detection algorithms. Among the much research (Wang et al., 2008, 2006; Li et al., 1998; Jia and Liu, 2004; Yi et al., 2013) on mesoscale eddies in the South China Sea, Nan et al. (2011) investigated three long-lived anticyclonic eddies (AE) in northern SCS 2007, two of which (named ACE2 and ACE3) experienced splitting and merging events during their evolution processes. So, this paper cites the two AEs as references to verify the detection results of the HD method and discusses the roles that multi-core structures play in eddies' evolution changes.

Figure 7 shows four consecutive snapshots of ACE3 during the merging event. According to Nan et al. (2011), one small eddy lasted for about 2 weeks and then merged into ACE3 on 22 August. In Fig. 7, a two-core structure were found near the Luzon Island on 8 August and the smaller component eddy close to the shore shrunk sharply but still remained in the composite structure after one week. On 22 August, the shrinking eddy disappeared and the two-core structure eventually turn into one-core eddy. So the evolvement episode of ACE3 recognized by HD is basically consistent with the descriptions in (Nan et al., 2011), except for the multi-core structure which provides detailed information (e.g. how the energy transfers) about the merging effect.

The other long-lived anticyclonic eddy ACE2, which split an small eddy on 11 July according to (Nan et al., 2011), is also examined, and Fig. 8 shows the evolution episode identified by the HD method during this splitting event. On 4 July, ACE2 constituted a two-core structure in a loose connection with ACE3. But one week later, they separated and ACE2 shrunk significantly. After then, ACE2 was strengthened judging by the core areas and constituted a more complex four-core structure on 18 July.

## Enhancing the accuracy of automatic eddy detection

J. Yi et al.

Title Page

Abstract

Introduction

Conclusions

References

Tables

Figures

⏪

⏩

◀

▶

Back

Close

Full Screen / Esc

Printer-friendly Version

Interactive Discussion



## Enhancing the accuracy of automatic eddy detection

J. Yi et al.

Title Page

Abstract

Introduction

Conclusions

References

Tables

Figures

◀

▶

◀

▶

Back

Close

Full Screen / Esc

Printer-friendly Version

Interactive Discussion

In addition, between ACE2 and ACE3 a small newborn eddy can be observed and expanded rapidly in the multi-core structure, which suggests that the evolvement of ACE2 and ACE3 had contributed much to the generation and the development of this internal newborn eddy.

Some differences can be observed in this detection result, especially that ACE2 was not found splitting a small eddy but rather separated with ACE3 between 4–11 July. Careful examinations reveal that this discrepancy mainly results from the different detection criteria we used in the HD method. Nan et al. employed the OW method to identify eddies so that they observed the splitting event since ACE2's core was indeed divided into two parts during that period. However, one part after the separation contained no SLA local maximum and was consequently excluded from HD's detection results. Despite such descriptive difference, our results well demonstrated the merit of recognizing the multi-core structures of eddies which explicitly unveil many evolution details (e.g. the generation of the newborn eddy between ACE2 and ACE3) that other detection algorithms can hardly obtain. It is an important improvement towards accurately tracking eddies' evolution and interacting dynamics. But it should be noted that multi-core structures only serve a good indicative of the complex relationships between eddies, and their authenticity requires further verifications.

## 4 Conclusions

This study proposed a new hybrid method, HD, which uses the SLA datasets to automatically identify the mesoscale eddies. The combination of detection criteria of the OW method and the SSH-based method effectively enhance the accuracy of eddy detection. And procedures are implemented in the HD method to fully recognize the multi-core structures of mesoscale eddies which serve the foundation of tracking eddies' dynamic events (e.g. splitting or merging) and eddies' mutual interactions during the evolution processes.

## Enhancing the accuracy of automatic eddy detection

J. Yi et al.

Title Page

Abstract

Introduction

Conclusions

References

Tables

Figures

⏪

⏩

◀

▶

Back

Close

Full Screen / Esc

Printer-friendly Version

Interactive Discussion

To objectively evaluate the detection accuracy of the HD method, this study adopted the validation protocol used by Chaigneau et al. (2008), and compared with the manual results detected by 5 experts. Ten random experiments in the South China Sea showed that the average successful detection rate was  $\sim 96.6\%$  and the excessive detection rate was  $\sim 14.2\%$ , which confirmed HD's improvement in detection accuracy. Second, the comparisons between different detection algorithms in the ESP study area well illustrated every method's performance as well as HD's capability of recognizing eddies' multi-core structures. Finally, by comparing with the long-lived anticyclonic eddies investigated by Nan et al. (2011), this study verified HD's detection results and found that the merging event happened to ACE3 was well recognized by HD while the discrepancy of ACE2's splitting event was mainly due to the different detection criteria between OW and HD. This detection verification well demonstrated the importance of recognizing the multi-core structures which facilitated identifying the splitting and merging dynamic changes and unveiled eddies evolving details that other detection algorithms can hardly achieve.

Currently, to automatically track eddies' splitting or merging dynamic changes remains a great challenge. And in the next paper, we will present the companion method of HD that attempts to tackle this challenge by incorporating a semantic model into the similarity-based eddy tracking algorithm.

*Acknowledgements.* This is a contribution to Research Project 41071250 of the National Science Foundation of China and 088RA500KA of the Innovation Projects of the State Key Laboratory of Resource and Environment Information System, Chinese Academy of Sciences. The altimeter products were produced by Ssalto/Duacs and distributed by Aviso, with support from Cnes (<http://www.aviso.oceanobs.com/duacs/>). We specially thank the experts for their manual detection of eddies for method validation.

## References

- Ari Sadarjoen, I. and Post, F. H.: Detection, quantification, and tracking of vortices using stream-line geometry, *Comput. Graph.*, 24, 333–341, doi:10.1016/s0097-8493(00)00029-7, 2000.
- Basdevant, C. and Philipovitch, T.: On the validity of the “Weiss criterion” in two-dimensional turbulence, *Physica D*, 73, 17–30, doi:10.1016/0167-2789(94)90222-4, 1994.
- Chaigneau, A. and Pizarro, O.: Eddy characteristics in the eastern South Pacific, *J. Geophys. Res.*, 110, C06005, doi:10.1029/2004jc002815, 2005.
- Chaigneau, A., Gizolme, A., and Grados, C.: Mesoscale eddies off Peru in altimeter records: identification algorithms and eddy spatio-temporal patterns, *Prog. Oceanogr.*, 79, 106–119, doi:10.1016/j.pocean.2008.10.013, 2008.
- Chelton, D. B. and Schlax, M. G.: The accuracies of smoothed sea surface height fields constructed from tandem satellite altimeter datasets, *J. Atmos. Ocean. Tech.*, 20, 1276–1302, doi:10.1175/1520-0426(2003)020<1276:taosss>2.0.co;2, 2003.
- Chelton, D. B., Schlax, M. G., Samelson, R. M., and de Szoeke, R. A.: Global observations of large oceanic eddies, *Geophys. Res. Lett.*, 34, L15606, doi:10.1029/2007gl030812, 2007.
- Chelton, D. B., Schlax, M. G., and Samelson, R. M.: Global observations of nonlinear mesoscale eddies, *Progress In Oceanography*, 91, 167–216, doi:10.1016/j.pocean.2011.01.002, 2011.
- Doglioli, A. M., Blanke, B., Speich, S., and Lapeyre, G.: Tracking coherent structures in a regional ocean model with wavelet analysis: application to Cape Basin eddies, *J. Geophys. Res.*, 112, C05043, doi:10.1029/2006jc003952, 2007.
- Dong, C., Liu, Y., Lumpkin, R., Lankhorst, M., Chen, D., McWilliams, J. C., and Guan, Y.: A scheme to identify loops from trajectories of oceanic surface drifters: an application in the Kuroshio extension region, *J. Atmos. Ocean. Tech.*, 28, 1167–1176, doi:10.1175/jtech-d-10-05028.1, 2011.
- Ducet, N., Le Traon, P. Y., and Reverdin, G.: Global high-resolution mapping of ocean circulation from TOPEX/Poseidon and ERS-1 and -2, *J. Geophys. Res.*, 105, 19477–19498, doi:10.1029/2000jc900063, 2000.
- Fang, F. and Morrow, R.: Evolution, movement and decay of warm-core Leeuwin Current eddies, *Deep-Sea Res. Pt. II*, 50, 2245–2261, doi:10.1016/s0967-0645(03)00055-9, 2003.
- Henson, S. A. and Thomas, A. C.: A census of oceanic anticyclonic eddies in the Gulf of Alaska, *Deep-Sea Res. Pt. I*, 55, 163–176, doi:10.1016/j.dsr.2007.11.005, 2008.

## Enhancing the accuracy of automatic eddy detection

J. Yi et al.

Title Page

Abstract

Introduction

Conclusions

References

Tables

Figures

⏪

⏩

◀

▶

Back

Close

Full Screen / Esc

Printer-friendly Version

Interactive Discussion



## Enhancing the accuracy of automatic eddy detection

J. Yi et al.

Title Page

Abstract

Introduction

Conclusions

References

Tables

Figures

⏪

⏩

◀

▶

Back

Close

Full Screen / Esc

Printer-friendly Version

Interactive Discussion



- Isern-Fontanet, J., Garcia-Ladona, E., and Font, J.: Identification of marine eddies from altimetric maps, 5, *American Meteorological Society, Boston, MA, ETATS-UNIS*, 7 pp., 2003a.
- Isern-Fontanet, J., Garcia-Ladona, E., and Font, J.: Identification of marine eddies from altimetric maps, *J. Atmos. Ocean. Tech.*, 20, 772–778, doi:doi:10.1175/1520-0426(2003)20<772:IOMEFA>2.0.CO;2, 2003b.
- Isern-Fontanet, J., Garcia-Ladona, E., and Font, J.: Vortices of the Mediterranean Sea: an altimetric perspective, *J. Phys. Oceanogr.*, 36, 87–103, doi:10.1175/JPO2826.1, 2006.
- Jia, Y. and Liu, Q.: Eddy shedding from the Kuroshio Bend at Luzon Strait, *J. Oceanogr.*, 60, 1063–1069, doi:10.1007/s10872-005-0014-6, 2004.
- Li, L., Nowlin Jr, W. D., and Jilan, S.: Anticyclonic rings from the Kuroshio in the South China Sea, *Deep-Sea Res. Pt. I*, 45, 1469–1482, doi:10.1016/s0967-0637(98)00026-0, 1998.
- McWilliams, J. C.: The nature and consequence of oceanic eddies, in: *Eddy-Resolving Ocean Modeling*, edited by: Hecht, M. and Hasumi, H., AGU Monograph, 5–15, 2008.
- Morrow, R., Birol, F., Griffin, D., and Sudre, J.: Divergent pathways of cyclonic and anti-cyclonic ocean eddies, *Geophys. Res. Lett.*, 31, L24311, doi:10.1029/2004gl020974, 2004.
- Nan, F., He, Z., Zhou, H., and Wang, D.: Three long-lived anticyclonic eddies in the northern South China Sea, *J. Geophys. Res.*, 116, C05002, doi:10.1029/2010jc006790, 2011.
- Nencioli, F., Dong, C., Dickey, T., Washburn, L., and McWilliams, J. C.: A vector geometry – based eddy detection algorithm and its application to a high-resolution numerical model product and high-frequency radar surface velocities in the Southern California Bight, *J. Atmos. Ocean. Tech.*, 27, 564–579, doi:10.1175/2009jtecho725.1, 2010.
- Okubo, A.: Horizontal dispersion of floatable particles in the vicinity of velocity singularities such as convergences, *Deep Sea Research and Oceanographic Abstracts*, 17, 445–454, doi:10.1016/0011-7471(70)90059-8, 1970.
- Pascual, A., Faugère, Y., Larnicol, G., and Le Traon, P.-Y.: Improved description of the ocean mesoscale variability by combining four satellite altimeters, *Geophys. Res. Lett.*, 33, L02611, doi:10.1029/2005gl024633, 2006.
- Penven, P., Echevin, V., Pasapera, J., Colas, F., and Tam, J.: Average circulation, seasonal cycle, and mesoscale dynamics of the Peru Current system: a modeling approach, *J. Geophys. Res.*, 110, C10021, doi:10.1029/2005jc002945, 2005.
- Traon, P. Y. L. and Dibarboure, G.: Mesoscale mapping capabilities of multiple-satellite altimeter missions, *J. Atmos. Ocean. Tech.*, 16, 1208–1223, doi:10.1175/1520-0426(1999)016<1208:MMCOMS>2.0.CO;2, 1999.

## Enhancing the accuracy of automatic eddy detection

J. Yi et al.

Title Page

Abstract

Introduction

Conclusions

References

Tables

Figures

⏪

⏩

◀

▶

Back

Close

Full Screen / Esc

Printer-friendly Version

Interactive Discussion



Wang, D., Xu, H., Lin, J., and Hu, J.: Anticyclonic eddies in the northeastern South China Sea during winter 2003/2004, *J. Oceanogr.*, 64, 925–935, doi:10.1007/s10872-008-0076-3, 2008.

Wang, G., Su, J., and Chu, P. C.: Mesoscale eddies in the South China Sea observed with altimeter data, *Geophys. Res. Lett.*, 30, 2121, doi:10.1029/2003gl018532, 2003.

Wang, G., Chen, D., and Su, J.: Generation and life cycle of the dipole in the South China Sea summer circulation, *J. Geophys. Res.*, 111, C06002, doi:10.1029/2005jc003314, 2006.

Weiss, J.: The dynamics of enstrophy transfer in two-dimensional hydrodynamics, *Physica D*, 48, 273–294, doi:10.1016/0167-2789(91)90088-q, 1991.

Xiu, P., Chai, F., Shi, L., Xue, H., and Chao, Y.: A census of eddy activities in the South China Sea during 1993–2007, *J. Geophys. Res.*, 115, C03012, doi:10.1029/2009jc005657, 2010.

Yi, J., Du, Y., Wang, X., He, Z., and Zhou, C.: A clustering analysis of eddies' spatial distribution in the South China Sea, *Ocean Sci.*, 9, 171–182, doi:10.5194/os-9-171-2013, 2013.

Yuan, D., Han, W., and Hu, D.: Surface Kuroshio path in the Luzon Strait area derived from satellite remote sensing data, *J. Geophys. Res.*, 111, C11007, doi:10.1029/2005jc003412, 2006.

## Enhancing the accuracy of automatic eddy detection

J. Yi et al.

**Table 1.** Accuracy evaluation results of the ten sample experiments on SLA maps.

	Date	1 13 Jul 1994	2 3 May 1995	3 17 Jul 1996	4 21 Jan 1998	5 8 Sep 1999	6 16 May 2001	7 9 Oct 2002	8 12 Nov 2003	9 11 May 2005	10 9 May 2007	Average
expert	Nc	23	23	18	19	17	26	25	19	22	25	21.7 ± 3.2
	RI (%)	8.7	36.5	31.1	21.1	15.3	20.7	16.0	16.8	20.9	20.0	20.7 ± 8.0
OW	SDR (%)	100.0	100.0	94.4	89.5	100.0	96.2	100.0	89.5	100.0	96.0	96.6 ± 4.3
	EDR (%)	69.9	47.8	77.7	89.5	64.7	38.5	56.0	100	54.5	104.0	70.3 ± 22.2
SLA extrema	SDR (%)	100.0	100.0	100.0	100.0	100.0	100.0	100.0	100.0	100.0	100.0	100.0 ± 0.0
	EDR (%)	17.4	30.4	83.3	42.1	58.8	30.8	16.0	21.1	31.8	36.0	36.8 ± 20.6
HD	SDR (%)	100.0	100.0	94.4	89.5	100.0	96.2	100.0	89.5	100.0	96.0	96.6 ± 4.3
	EDR (%)	8.7	21.7	22.2	10.6	17.6	7.7	4.0	10.6	22.7	16.0	14.2 ± 6.7

Title Page

Abstract

Introduction

Conclusions

References

Tables

Figures

⏪

⏩

◀

▶

Back

Close

Full Screen / Esc

Printer-friendly Version

Interactive Discussion



## Enhancing the accuracy of automatic eddy detection

J. Yi et al.

### Step 1: identification of eddy centers

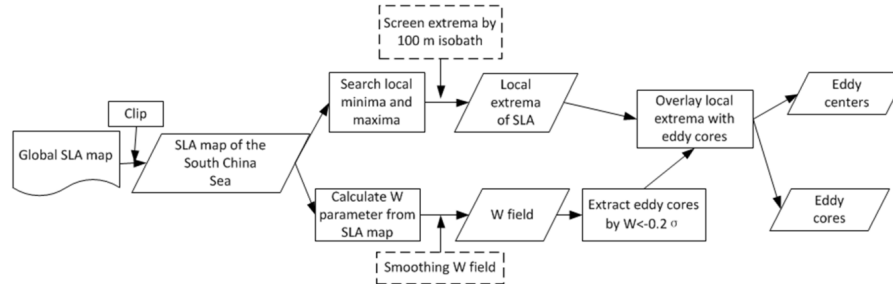


**Fig. 1.** Detailed procedures of step 1. Procedure in the box with dashed border is adaptable according to the data quality and the eddy characteristics of different study regions.

Title Page

Abstract

Introduction

Conclusions

References

Tables

Figures

⏪

⏩

◀

▶

Back

Close

Full Screen / Esc

Printer-friendly Version

Interactive Discussion



## Enhancing the accuracy of automatic eddy detection

J. Yi et al.

### Step 2: extraction of eddy boundaries

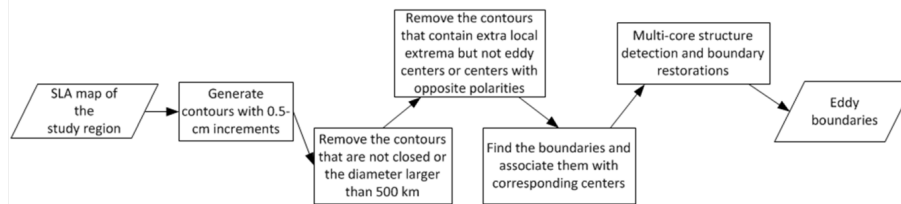


**Fig. 2.** Detailed procedures of step 2.

Title Page

Abstract

Introduction

Conclusions

References

Tables

Figures

⏪

⏩

◀

▶

Back

Close

Full Screen / Esc

Printer-friendly Version

Interactive Discussion

## Enhancing the accuracy of automatic eddy detection

J. Yi et al.

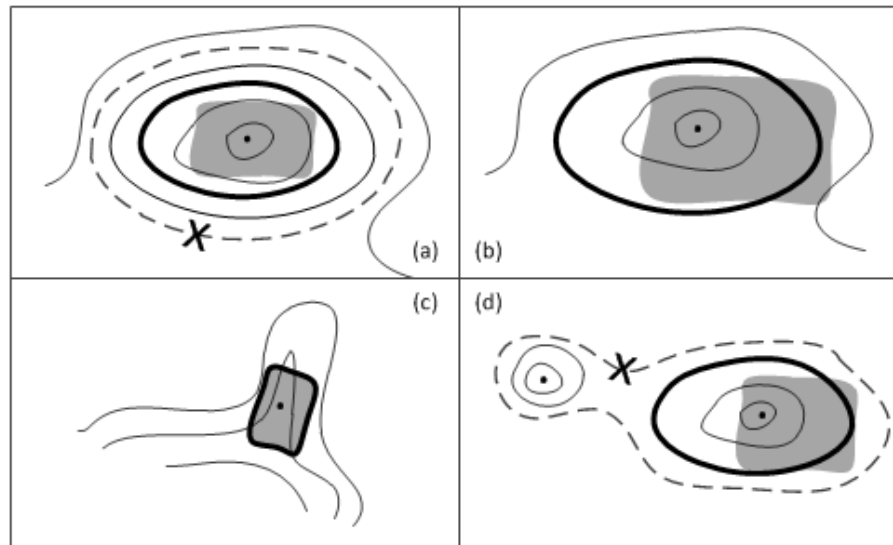


**Fig. 3.** Possible situations in extracting eddy boundary. The contours are represented by the thin solid lines while the eddy boundary is underlined by the thick solid line. Eddies' core areas are symbolized by grey polygons. And the dashed lines denote the outmost closed contours.

Title Page

Abstract

Introduction

Conclusions

References

Tables

Figures

⏪

⏩

◀

▶

Back

Close

Full Screen / Esc

Printer-friendly Version

Interactive Discussion



## Enhancing the accuracy of automatic eddy detection

J. Yi et al.

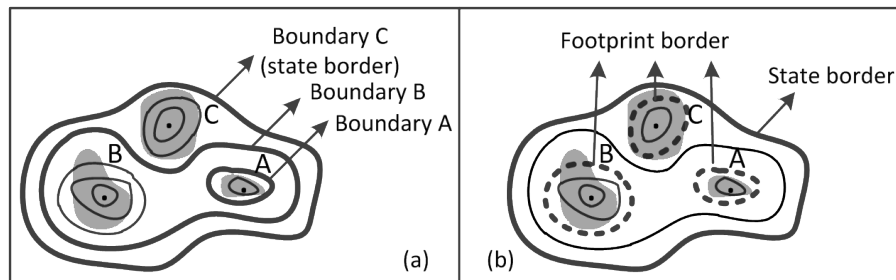


**Fig. 4.** Identification of multi-core structures and boundary restorations. The contours are represented by thin solid lines. The grey polygons represent eddies' core areas.

Title Page

Abstract

Introduction

Conclusions

References

Tables

Figures

◀

▶

◀

▶

Back

Close

Full Screen / Esc

Printer-friendly Version

Interactive Discussion

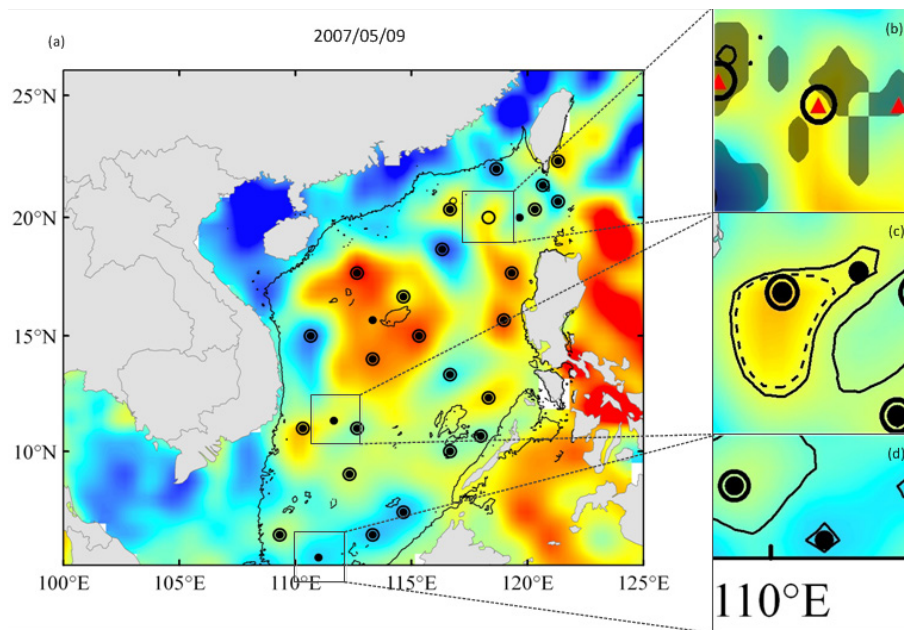


**Fig. 5.** Comparisons between experts' detection result and HD's result on 9 May 2007. **(a)** The 100 m depth isobath is delineated by the black solid line. The circles represent eddies identified by experts while the dots represent the ones identified by HD. **(b)** One missed eddy in HD's result. Red triangles represent the SLA local extrema, and the grey polygons represent eddies' core areas. **(c)** One over-detected eddy that constitutes a multi-core structure. The state borders are delineated by the solid lines and the footprint borders by the dashed lines. **(d)** The other over-detected eddy located near the border of study region.

## Enhancing the accuracy of automatic eddy detection

J. Yi et al.

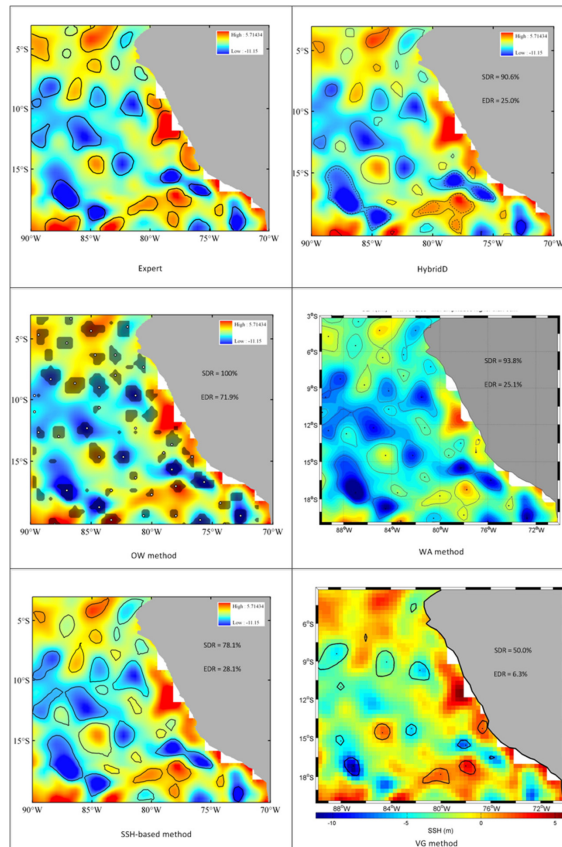


**Fig. 6.** Results of manual detection and automatic algorithms. The boundaries are delineated by black solid lines. Grey dark polygons in the OW detection denote where  $W$  parameter satisfies the criterion, and the white dots are the SLA local extrema.

[Title Page](#)
[Abstract](#)
[Introduction](#)
[Conclusions](#)
[References](#)
[Tables](#)
[Figures](#)
[⏪](#)
[⏩](#)
[⏴](#)
[⏵](#)
[Back](#)
[Close](#)
[Full Screen / Esc](#)
[Printer-friendly Version](#)
[Interactive Discussion](#)

## Enhancing the accuracy of automatic eddy detection

J. Yi et al.

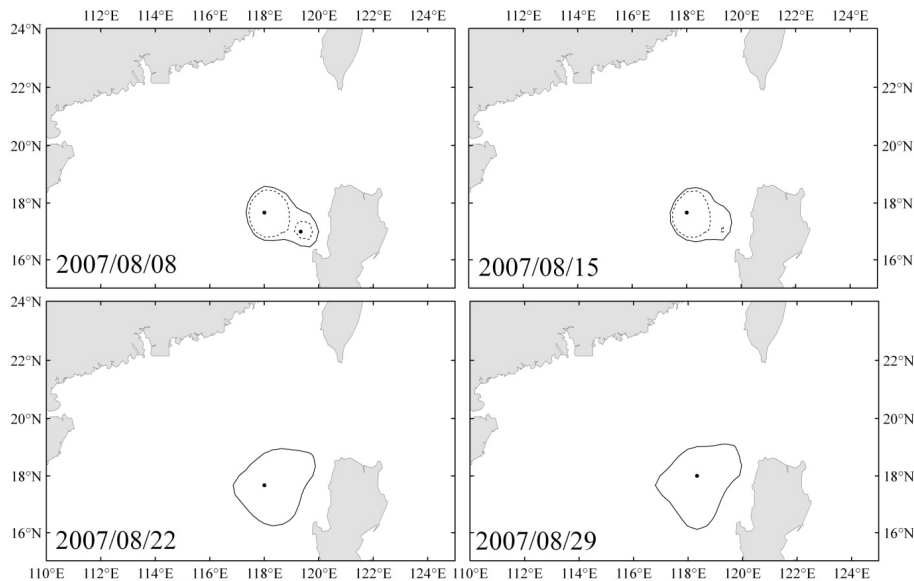


**Fig. 7.** Evolution snapshots of ACE3's merging event. The state border is delineated by the solid line while the footprint border is delineated by the dashed line.

[Title Page](#)[Abstract](#)[Introduction](#)[Conclusions](#)[References](#)[Tables](#)[Figures](#)[⏪](#)[⏩](#)[◀](#)[▶](#)[Back](#)[Close](#)[Full Screen / Esc](#)[Printer-friendly Version](#)[Interactive Discussion](#)

## Enhancing the accuracy of automatic eddy detection

J. Yi et al.

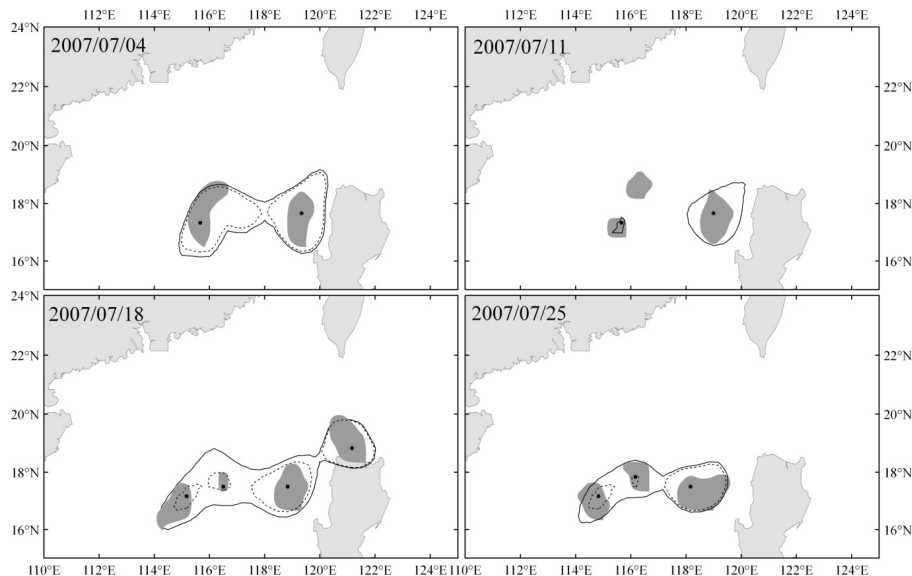


**Fig. 8.** evolution snapshots of ACE2's splitting event. The dots represent eddy centers while the dark grey polygons represent eddies' core areas. The state border is delineated by the solid line while the footprint border is delineated by the dashed line.

[Title Page](#)[Abstract](#)[Introduction](#)[Conclusions](#)[References](#)[Tables](#)[Figures](#)[⏪](#)[⏩](#)[◀](#)[▶](#)[Back](#)[Close](#)[Full Screen / Esc](#)[Printer-friendly Version](#)[Interactive Discussion](#)